Growth of needle-shaped crystals in the presence of convection

D. A. Saville and P. J. Beaghton
Department of Chemical Engineering, Princeton University, Princeton, New Jersey 08544
(Received 24 August 1987)

The motion of the freezing front between a needle-shaped crystal and a supercooled liquid is analyzed for situations where there is forced convection aligned with the crystal axis. It is shown that in the absence of capillary effects the shape of the crystal-melt interface is a paraboloid of revolution, similar to that found in situations where diffusion is the sole heat-transfer mechanism. A relation between the supercooling, the product of tip velocity and tip radius, and the strength of the flow is derived which reduces to the well-known Ivantsov theory in the absence of convection.

I. INTRODUCTION

The interrelation between nonequilibrium systems and complex growth forms was recognized long ago,[1] but during the past decade interest in pattern formation has been particularly intense. Dendritic growth, the formation of branched, treelike structures when an interface advances into a metastable phase, has received special attention because of its technological importance. Unfortunately, understanding phenomena as common as this is hampered by their mathematical complexity. Although the theoretical model resembles the classical Stefan problem wherein the diffusion equation describes the transport process, there are important differences. For example, the local temperature of a nonplanar freezing front deviates from the melting point of a flat interface due to curvature—the Gibbs-Thompson effect. In addition, fluid motion complicates the problem by adding convective transport to the energy balance.

Ivantsov's theory,[2] a cornerstone of our understanding of dendritic growth, deals with situations where fluid motion and surface tension are absent. His theory describes uniformly propagating "needle crystals" in the form of isothermal paraboloids of revolution (or parabolas in two dimensions) advancing into a subcooled liquid. It yields a single relation between the dimensionless supercooling $\Delta \equiv (T_M - T_\infty)c_p/L$ and the Péclet number $p \equiv \rho V/2\alpha$. The Péclet number involves the tip radius ρ, the tip velocity V, and α, the heat diffusivity of the melt. The difference between the melting temperature T_M and the bulk temperature T_∞ is scaled with the latent heat of fusion L and the heat capacity c_p.

The Ivantsov family of solutions is *degenerate:* for a given supercooling there exist an infinite number of paraboidal shapes; only the product of the tip velocity and tip radius appears in the theory. Furthermore, linear-stability analysis shows that the Ivantsov paraboloids are unstable to infinitesimal perturbations. The indeterminacy can be removed by introducing the effects of surface tension. According to the Gibbs-Thompson equation, the (dimensionless) temperature of the solid-liquid interface is given by $\Delta - (d_0/l)\kappa$, where κ is the dimensionless local curvature, d_0 is a capillary length proportional to the solid-liquid interfacial energy or surface tension, and l is an appropriate length scale. The first analysis of the effects of surface tension used the Ivantsov solution as a basic state and treated the capillary term in the Gibbs-Thompson boundary condition as a regular perturbation. For values of $d_0/(p\rho)$ $(\equiv\sigma)$ larger than a critical value σ^*, a continuous family of stable, modified Ivantsov dendrites was found. Accordingly, the operating point for the dendrite is determined by the marginally stable solution $\sigma = \sigma^*$. A comprehensive review of the subject is Langer's 1980 article.[3]

Recent studies have focused on the subtle influence of surface tension on the mathematical structure of the problem. Since the capillary length is several orders of magnitude smaller than the tip radius, the steady-state correction to the Ivantsov solution in the presence of surface tension is negligibly small. However, the curvature operator contains higher-order derivatives which are multiplied by a small parameter and this presents a singular perturbation problem. A theory of microscopic solvability has been developed to describe the dynamics of diffusion-controlled growth in the presence of capillary effects.[4–8]

Despite its limitations, the Ivantsov theory remains a valuable starting point and it accurately predicts the relationship between supercooling and Péclet number for *moderate* to *large* supercoolings. Furthermore, the shape of a real dendritic tip is unmistakably paraboloidal, as in the Ivantsov theory. However, at low supercoolings there is a strong deviation from the Ivantsov theory due to convection. Even under carefully controlled experimental conditions, thermal gradients in the melt generate buoyancy-driven flows which disturb the diffusion-dominated temperature profiles. Experiments by Glicksman and Huang[9] show that natural convection alters the morphology of the crystal and the relationship between growth rate and undercooling.

Stimulated by these experimental results, we constructed a complement to Ivantsov's theory to provide a basis for more detailed investigations where convection is present. In natural convection the temperature field is coupled to the equation of motion through the buoyancy term, which makes the problem all but intractable for

most interface shapes unless one resorts to numerical methods to solve the partial differential equations. Thus, a simpler flow is needed to express the salient effects of convection on the solidification front. This led us to consider forced convection past a paraboloid of revolution.[10]

The velocity field used here is that for flow directed parallel to the axis of a paraboloidal crystal. An exact solution to the equations of motion in the Oseen approximation is used to represent the flow so viscous and pressure forces are balanced with a small contribution from inertia. In Sec. II we analyze the integral equation that represents the interface temperature in terms of interface shape and the temperature and velocity fields in the liquid. Capillary effects are ignored so the interface is isothermal. We show that uniformly translating paraboloidal solidification fronts are admissible solutions. Then an expression is given relating the undercooling to the freezing velocity and the strength of the flow. Some numerical results and conclusions are discussed in Sec. III. A derivation of the integral equation describing interface motion when convection is present is given in the Appendix. Since we rely heavily on the work of others in this matter, only a bare outline is necessary.

II. THEORY

We consider the steady uniform propagation of an isothermal solid-liquid interface with a constant freezing velocity Vi_z as illustrated in Fig. 1. Densities of solid and liquid are assumed to be identical. In a frame of reference traveling with the front velocity V, the steady temperature field in the subcooled liquid is governed by the convective-diffusion equation

$$\alpha\tilde{\nabla}^2\tilde{T}+V\frac{\partial\tilde{T}}{\partial\tilde{z}}=\tilde{\mathbf{v}}\cdot\tilde{\nabla}\tilde{T}\ , \tag{2.1}$$

where $\tilde{\mathbf{v}}$ is a steady flow field that satisfies the incompressible Navier-Stokes equation and the no-slip and mass conservation conditions on the solid-liquid interface. Since interface motion does not generate convection unless there is a density difference between the solid and liquid phase, $\tilde{\mathbf{v}}=0$ in the absence of an externally imposed flow.

Here we neglect the effect of surface tension and the entire solid is assumed to be at its melting temperature T_M, while the bulk liquid phase is supercooled to T_∞. The heat conservation condition at the interface $\tilde{z}=\tilde{\zeta}(\tilde{x},\tilde{y})$ is

$$\frac{L}{c_p}Vn_{\tilde{z}}=-\alpha\tilde{\nabla}\tilde{T}\cdot\hat{\mathbf{n}}\ , \tag{2.2}$$

where $\hat{\mathbf{n}}$ is the outward unit normal with $n_{\tilde{z}}$ as its $\tilde{z}$ component.

Next, introduce a dimensionless temperature $T=(\tilde{T}-T_\infty)c_p/L$ and scale the lengths with $2\alpha/V$. In terms of dimensionless variables the equations are

$$\nabla^2T+2\frac{\partial T}{\partial z}=2\lambda\mathbf{v}\cdot\nabla T\ , \tag{2.3}$$

$$\nabla T\cdot\hat{\mathbf{n}}\,|_{z=\zeta(x,y)}=-2n_z\ , \tag{2.4}$$

$$T\,|_{z=\zeta(x,y)}=\Delta\ , \tag{2.5}$$

where $\lambda=U_\infty/V$; U_∞ represents the characteristic flow velocity. The interface $z=\zeta(x,y)$ and the solid are now at the temperature $\Delta\equiv(T_M-T_\infty)c_p/L$ (the dimensionless supercooling), whereas the dimensionless temperature goes to zero as $z\to\infty$.

Equations (2.3)–(2.5) are equivalent to the following integral equation for the interface shape $\zeta(x,y,)$ (the derivation is sketched in the Appendix):

$$\Delta=\int_{-\infty}^{\infty}dx'\int_{-\infty}^{\infty}dy'2G_{ss}(\mathbf{x}_\Gamma,\mathbf{x}'_\Gamma)-\lambda\int_{-\infty}^{\infty}dx'\int_{-\infty}^{\infty}dy'\int_{\zeta(x',y')}^{\infty}dz'2G_{ss}(\mathbf{x}_\Gamma,\mathbf{x}')\times\mathbf{v}(\mathbf{x}')\cdot\nabla T(\mathbf{x}')\ , \tag{2.6}$$

where $\mathbf{x}=(x,y,z)$ and $\mathbf{x}_\Gamma=(x,y,\zeta(x,y))$. $G_{ss}(\mathbf{x},\mathbf{x}')$ denotes the Green's function corresponding to steady heat diffusion due to a point source at $\mathbf{x}$ in the reference frame moving with velocity V. In the pure diffusion problem $\lambda=0$, so the temperature field is represented by an integral superposition of point-heat sources along the solid-liquid interface ζ. The boundary temperature Δ can then be expressed in terms of two-dimensional integrals.

In contrast to the pure diffusion case, the integral representation of the convective-diffusion equation involves integrating over the entire fluid domain, the second term on the right-hand side of (2.6). This increase in the dimensionality of the integral equation is due to the lack

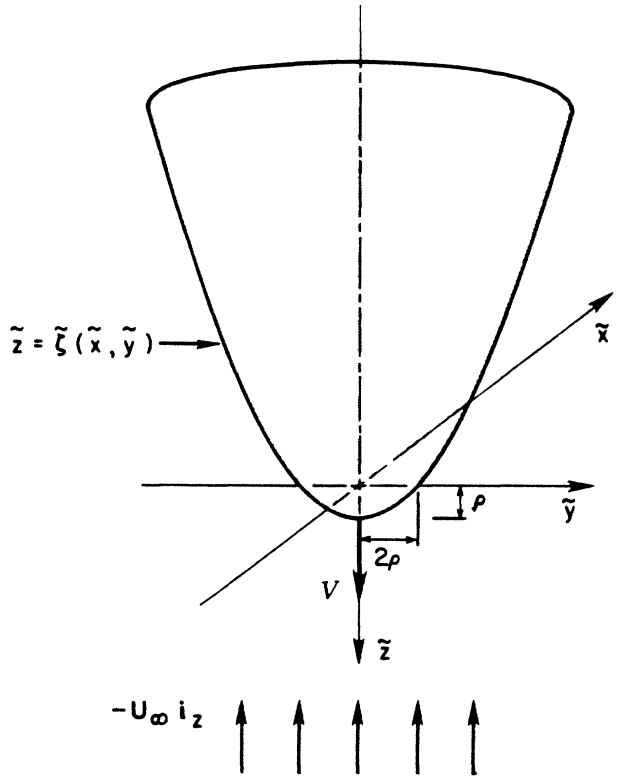

FIG. 1. Diagram of the coordinate system showing the orientation of the paraboloidal crystal and the flow.

of appropriate Green's functions for partial differential equations with variable coefficients. Nevertheless, a scheme based on the integral formulation has many advantages over other methods even when there is flow in the melt.

The integral expression is now used to search for uniformly translating interface shapes in the presence of fluid flow. Experiments in the "convective" regime (low supercoolings) suggest that the tip region remains paraboloidal even when the characteristic flow velocity is much larger than the freezing velocity. Thus we look for a class of temperature fields (and the corresponding flow fields) that satisfies the integral expression in cases where the interface is paraboloidal, viz.,

$$z=\zeta(x,y)=\frac{p}{2}\left[1-\frac{x^2+y^2}{p^2}\right] . \tag{2.7}$$

Here the Péclet number p can be viewed as the dimensionless radius of curvature at the tip of the paraboloid.

We pattern our search for interface shapes after Pelce and Pomeau,[11] who used elementary variable transformations to show that the integral

$$\int_{-\infty}^{\infty} dx' \int_{-\infty}^{\infty} dy' 2G_{ss}(\mathbf{x},\mathbf{x}')$$

is *independent* of $\mathbf{x}=(x,y,z)$ if both $\mathbf{x}$ and $\mathbf{x}'$ represent points on the same paraboloidal interface ζ, i.e., $\mathbf{x}=(x,y,\zeta(x,y))$ and $\mathbf{x}'=(x',y',\zeta(x',y'))$. Their result was used to demonstrate that the Ivantsov paraboloid is a solution of the diffusion equation and it can be easily extended to show that the integral is independent of $\mathbf{x}$ when $\mathbf{x}$ and $\mathbf{x}'$ represent points on two different confocal paraboloids, such as those represented by (2.7) for two different Péclet numbers. Using this extension of Pelce and Pomeau's result, we can produce temperature fields compatible with a paraboloidal interface shape. Since the left-hand side of Eq. (2.6) is constant, one must show that the right-hand side can be independent of $\mathbf{x}_\Gamma$ under certain assumptions about the nature of the temperature and flow fields. Pelce and Pomeau have already disposed of the first term. To complete the demonstration, the second integral, which comes from the convective term of the governing equation, must be shown to be independent of the position vector $\mathbf{x}_\Gamma$ as $\mathbf{x}_\Gamma$ traverses the paraboloid interface.

Let I_c stand for the second integral expression in (2.6). Then, since paraboloidal shapes are under study, it is convenient to introduce a paraboloidal coordinate system,

$$w=\frac{z+(x^2+y^2+z^2)^{1/2}}{p} ,$$

$$s=\frac{-z+(x^2+y^2+z^2)^{1/2}}{p} ,$$

$$\phi=\arctan\frac{y}{x} .$$

In this new coordinate system the interface defined by (2.7) is represented by the surface $w=1$; $z\to\infty$ is equivalent to $w\to\infty$. Conversely, the surface $w=a$ represents a paraboloid confocal to $w=1$ with a dimensionless tip radius $p'=ap$. The integral I_c becomes

$$I_c=\int_0^{2\pi} d\varphi' \int_0^{\infty} ds' \int_{w'=1}^{\infty} dw' p'^3 \frac{s'+w'}{2} G_{ss}(\mathbf{x}_\Gamma,\mathbf{x}') \times \mathbf{v}(\mathbf{x}')\cdot\nabla T(\mathbf{x}') . \tag{2.8}$$

If

$$p'^3\frac{s'+w'}{2}\mathbf{v}(\mathbf{x}')\cdot\nabla T(\mathbf{x}')\equiv \hat{A}(s',\varphi',w') \tag{2.9}$$

were only a function of w' (this will be shown to be true for a certain class of flows later), then (2.8) could be rewritten as

$$I_c=\int_{w'=1}^{\infty} dw' \hat{A}(w') \int_0^{2\pi} d\varphi' \int_0^{\infty} ds' G_{ss}(\mathbf{x}_\Gamma,\mathbf{x}') . \tag{2.10}$$

Once this is done, the integrals with respect to ϕ' and s' can be rewritten in terms of x' and y' and (2.10) becomes

$$I_c=\int_{w'=1}^{\infty} dw' A(w') \int_{-\infty}^{\infty} dx' \int_{-\infty}^{\infty} dy' G_{ss}(\mathbf{x}_\Gamma,\mathbf{x}') , \tag{2.11}$$

where

$$A(w')=\frac{2}{p^2 w'}\hat{A}(w') ,$$

$$\mathbf{x}'=(s',\varphi',w')=\left[x',y',z'=\frac{pw'}{2}\left[1-\frac{x'^2+y'^2}{(pw')^2}\right]\right]$$

and

$$\mathbf{x}_\Gamma=(s,\varphi,w=1)=\left[x,y,z=\frac{p}{2}\left[1-\frac{x^2+y^2}{p^2}\right]\right] .$$

For every value of w', $\mathbf{x}'$ and $\mathbf{x}_\Gamma$ represent two confocal paraboloids with a ratio of tip radii equal to w'. The extended result of Pelce and Pomeau therefore applies directly to the integrals over x' and y' in (2.11), i.e., for a given paraboloidal surface w' the integral does not depend on $\mathbf{x}_\Gamma$ as it moves along that surface. A final integration with respect to w' shows that the convective integral in (2.6) is independent of the interface position vector $\mathbf{x}_\Gamma$ (which represents the paraboloidal surface ζ) as long as the quantity $A(s',\varphi',w')$ is a function of w' alone. Note that in the paraboloidal coordinate system, A can be written as

$$A=2\sqrt{(w'+s')}\left[\sqrt{w'}v_w\frac{\partial T}{\partial w'}+\sqrt{s'}v_s\frac{\partial T}{\partial s'} + \left[\frac{(w'+s')}{4w's'}\right]^{1/2} v_\varphi\frac{\partial T}{\partial\varphi'}\right] . \tag{2.12}$$

To identify a situation where $A(s',\phi',w')$ is independent of s' and ϕ', consider the uniform propagation of a paraboloidal freezing front in the presence of a flow field with a uniform far-field velocity in the direction of the axis of the paraboloid, shown in Fig. 1. The fluid velocity $\bar{\mathbf{v}}$ satisfies the no-slip condition on the solid-liquid interface.

Uniform flow past paraboloids of revolution[12] or parabolas, in two dimensions, has been studied by a number of authors. Davis and Werle[13] showed that the solution to the Oseen equation

$$-\frac{2\lambda}{\mathcal{P}}\frac{\partial \mathbf{v}}{\partial z}=-\nabla P+\nabla^2\mathbf{v} \tag{2.13}$$

is a uniformly valid approximation to solutions of the Navier-Stokes equations for small Reynolds numbers, $\mathcal{R}\equiv\rho U_\infty/\nu=2p\lambda/\mathcal{P}$, where ν is the kinematic viscosity and $\mathcal{P}\equiv\nu/\alpha$ is the Prandtl number. Note, however, that the solution to the Oseen equation is not uniformly valid for planar flows. Wilkinson[14] derived an analytical expression for the Oseen velocity $\mathbf{v}=(v_w,v_s,v_\phi)$ past a paraboloid in a uniform stream parallel to its axis. In paraboloidal coordinates the velocity is

$$v_w=\frac{1}{\sqrt{w+s}}\left[\frac{e^{-\Lambda}-e^{-\Lambda w}}{\Lambda\sqrt{w}E_1(\Lambda)}+\sqrt{w}\,\frac{E_1(\Lambda w)-E_1(\Lambda)}{E_1(\Lambda)}\right], \tag{2.14a}$$

$$v_s=-\frac{\sqrt{s}}{\sqrt{w+s}}\,\frac{E_1(\Lambda w)-E_1(\Lambda)}{E_1(\Lambda)}, \tag{2.14b}$$

$$v_\phi=0, \tag{2.14c}$$

where E_1 is the exponential integral of first order and $\Lambda=\lambda p/\mathcal{P}$. On the surface $w=1$ $(z=\xi)$, $v_w=v_s=0$, whereas for $w\to\infty$ $(z\to\infty)$, $v_w=-1$ and $v_s=0$.

Now we introduce paraboloidal coordinates yielding

$$w\frac{\partial^2 T}{\partial w^2}+s\frac{\partial^2 T}{\partial s^2}+[1+pw-\lambda p\sqrt{w(w+s)}v_w]\frac{\partial T}{\partial w}+[1-ps-\lambda p\sqrt{s(w+s)}v_s]\frac{\partial T}{\partial s}=0, \tag{2.15}$$

$$\left.\frac{\partial T}{\partial w}\right|_{w=1}=-p, \tag{2.16}$$

$$T|_{w=1}=\Delta \tag{2.17}$$

for axisymmetric temperature fields. Equation (2.15) can be combined with Eq. (2.12) to give

$$w\frac{\partial^2 T}{\partial w^2}+s\frac{\partial^2 T}{\partial s^2}+(1+pw)\frac{\partial T}{\partial w}+(1-ps)\frac{\partial T}{\partial s}=\frac{p\lambda}{2}A(w,s). \tag{2.18}$$

For a paraboloidal solidification front, $A(w,s)$ and $T(w,s)$ must be independent of s. It is readily shown that $T=T(w)$ will satisfy Eqs. (2.16)–(2.18) with the velocity field represented by (2.14), so here $A=A(w)$.

Now (2.15) can be integrated analytically to give the derivative of the temperature with respect to the normal coordinate w, i.e.,

$$\frac{\partial T}{\partial w}=-p\exp\left[p(1-w)(1+\lambda)+\left[-1+\frac{\mathcal{P}e^{-\Lambda}}{E_1(\Lambda)}\right]\ln w+\frac{\mathcal{P}}{E_1(\Lambda)}[-E_1(\Lambda)+E_1(\Lambda w)+E_2(\Lambda)-E_2(\Lambda w)]\right], \tag{2.19}$$

where E_1 and E_2 are the exponential integrals of first and second order, respectively. One more integration gives the surface temperature of the crystal, viz.,

$$\Delta=-\int_{w=1}^{\infty}dw\frac{\partial T}{\partial w}=\int_{w=1}^{\infty}dw\,p\exp\left[p(1-w)(1+\lambda)+\left[-1+\frac{\mathcal{P}e^{-\Lambda}}{E_1(\Lambda)}\right]\ln w+\frac{\mathcal{P}}{E_1(\Lambda)}[-E_1(\Lambda)+E_1(\Lambda w)+E_2(\Lambda)-E_2(\Lambda w)]\right]. \tag{2.20}$$

Recall that $\Lambda\equiv\lambda p/\mathcal{P}$.

At this point we have derived a relation between the supercooling and Péclet number for a paraboloidal crystal formed by freezing a supercooled melt in the presence of convection, viz.,

$$\Delta=\Delta(p,\lambda,\mathcal{P}). \tag{2.21}$$

Two new parameters are involved: a Prandtl number, ν/α, and the ratio of the velocity of the flow to the freezing velocity, λ. The relation is more complicated than that derived by Ivantsov for pure diffusion in that the convective velocity and the viscosity of the melt are involved. Furthermore, the parameter λ depends on the supercooling through V.

III. CONCLUSIONS

The introduction of convective heat transfer into the equations governing dendritic growth has been shown to leave the paraboloidal shape intact when the flow structure has a certain form. This form derives from a solution to the viscous flow equations describing the interaction of a single axisymmetric dendrite with a uniform flow when the flow is slow, i.e., in the Oseen approximation. This sort of convection leads to a new family of needle crystals whose growth velocity is appropriately modified.

To illustrate the degree to which convection alters the relation between the Péclet number and undercooling, some representative calculations using the properties of succinonitrile are presented in Fig. 2. As the figure indicates, forced convection increases the solidification rate substantially when the characteristic flow velocity is large compared to the solidification velocity. For example, at a dimensionless undercooling of 0.002, the Péclet number with a velocity ratio of 50 is almost twice the Ivantsov value. To emphasize that this is a very weak flow by ordinary standards we cite some results from experiments

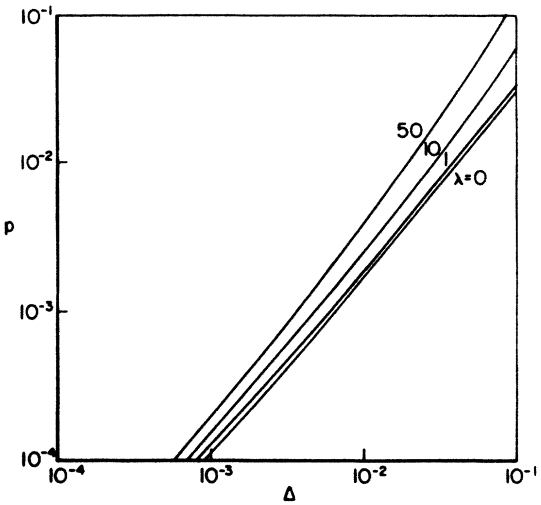

FIG. 2. The Péclet number as a function of undercooling for selected values of the velocity ratio. For these calculations the Prandtl number is 23.2 (succinonitrile). The Ivantsov solution corresponds to $\lambda=0$.

at low undercoolings.

At a dimensionless supercooling of 0.002, Glicksman and Huang[9] found the growth velocity to be roughly 0.8 μm per second and a velocity fifty times this is only 40 μm per second which, as the following scale analysis shows, can easily arise from buoyancy. The actual structure of the dendritic mass that generated flow in the experiments is not known but, as noted by Glicksman and Huang,[9] it is larger than the radius of an individual tip. Accordingly, each dendritic arm is immersed in a flow field configured by the entire dendritic mass. A representative velocity in a weak flow generated by natural convection is proportional to the characteristic temperature difference and the square of a characteristic length. In this case we can write it as

$$U_\infty=\frac{g\beta L}{c_p\nu}\Delta l^2 , \tag{3.1}$$

where g is the acceleration due to gravity, β is the coefficient of thermal expansion, and l is a characteristic length for the dendritic mass. Using the properties of succinonitrile, we find

$$U_\infty=740\Delta l^2 \text{ cm/s} ,$$

with l measured in centimeters. Accordingly, a dendritic mass with a characteristic length of a little over half a millimeter would generate a 40 μm per second flow at an undercooling of 0.002. Nevertheless, the obvious differences between free and forced convection are enough to deter us from delving further into the experimental results until the detailed structure of free convection for this situation has been worked out.

The theory advanced here makes no allowance for the effects of surface tension which we know has a profound effect on the details of dendritic growth. However, this work provides the necessary starting point for adapting more detailed theories to include convective effects which, according to the experimental results on succinonitrile, are quite important. In work to be reported shortly, we developed a nonlinear scheme which tracks the evolution of an axisymmetric interface. By solving the transient counterpart of (2.6) numerically, we find that the interface is unstable to finite amplitude disturbances.

ACKNOWLEDGMENT

This work was supported by NASA Microgravity Science and Applications Division under Grant No. NAG 3-447 administered through the Lewis Research Center.

APPENDIX: DERIVATION OF THE INTEGRAL EQUATION

In this appendix we sketch the derivation of the equation that describes the evolution of the dendritic interface. Langer and his colleagues[3,4,15] have given the essential mathematical steps, so adding convection is straightforward if we build on their work. The salient features are given here to make our presentation reasonably self-contained. The convective-diffusion equation is first written in differential form

$$\frac{\partial\tilde{T}}{\partial\tilde{t}}+\tilde{\mathbf{v}}\cdot\tilde{\nabla}_{\tilde{\mathbf{x}}}\tilde{T}-\alpha\tilde{\nabla}^2_{\tilde{\mathbf{x}}}\tilde{T}-V\frac{\partial\tilde{T}}{\partial\tilde{z}}=0 , \tag{A1}$$

where $\tilde{\mathbf{x}}=(\tilde{x},\tilde{y},\tilde{z})=(\tilde{\mathbf{r}},\tilde{z})=(\tilde{r},\tilde{\varphi},\tilde{z})$, α is the thermal diffusivity, and $V\mathbf{i}_z$ is the constant velocity of the moving coordinate system. The hydrodynamic velocity field $\tilde{\mathbf{v}}$ satisfies the no-slip condition on the interface and is zero in the solid. Under the assumptions of the two-sided model proposed by Langer,[15] the thermal diffusivities and the densities of the two phases are considered equal. We scale lengths with $2\alpha/V$ and time with $4\alpha/V^2$

$$\frac{\partial T}{\partial t}+2\lambda\mathbf{v}\cdot\nabla_{\mathbf{x}}T-\nabla^2_{\mathbf{x}}T-2\frac{\partial T}{\partial z}=0 , \tag{A2}$$

where $\lambda\equiv U_\infty/V$ is the ratio of the characteristic fluid velocity scale to the velocity of the coordinate system. The temperature field vanishes as $z\to\infty$ and

$$\lim_{z\to\pm\infty}T(\mathbf{x},t)=\text{const} . \tag{A3}$$

The temperature also satisfies the thermodynamic boundary condition

$$T_\Gamma=\Delta-\epsilon\kappa , \tag{A4}$$

with $T=(\tilde{T}-T_\infty)c_p/L$ and $\epsilon\equiv d_0V/2\alpha$; κ is the dimensionless curvature. Finally, heat conservation at the interface requires that

$$\hat{\mathbf{n}}\cdot\nabla_{\mathbf{x}}T_{\text{liquid}}-\hat{\mathbf{n}}\cdot\nabla_{\mathbf{x}}T_{\text{solid}}=-[2+\dot{\zeta}(\mathbf{r},t)]\hat{\mathbf{n}}\cdot\mathbf{i}_z . \tag{A5}$$

We now introduce the fundamental solution $G(\mathbf{x},\mathbf{x}';t-t')$ of the transient diffusion equation in an unbounded domain; in the moving coordinate system it is defined by

$$\frac{\partial G}{\partial t'}-\nabla^2_{\mathbf{x}'}G-2\frac{\partial G}{\partial z'}=-\delta(\mathbf{x}-\mathbf{x}')\delta(t-t') \tag{A6}$$

and $G(\mathbf{x},\mathbf{x}';t-t')\equiv0$ for $t<t'$. The fundamental solution (or Green's function) is

$$G(\mathbf{x},\mathbf{x};t-t')=\frac{H(t-t')}{[4\pi(t-t')]^{3/2}}\exp\left[-\frac{|\mathbf{r}-\mathbf{r}'|^2+[z-z'+2(t-t')]^2}{4(t-t')}\right], \tag{A7}$$

where $H(t-t')$ is Heaviside's step function. By taking the Fourier transform of (A6) Langer[15] derived the following integral representation of $G(\mathbf{x},\mathbf{x}';t-t')$:

$$G(\mathbf{x},\mathbf{x}';t-t')=\int_{-\infty}^{\infty}\frac{d\omega}{2\pi}\int\frac{d\mathbf{k}}{(2\pi)^3}\frac{e^{i\omega(t-t')+i\mathbf{k}\cdot(\mathbf{x}-\mathbf{x}')}}{i\omega+k^2-2ik_z}. \tag{A8}$$

Following the notation of Caroli *et al.*,[4] we define $t_-\equiv\lim_{c\to 0+}(t-c)$. Then

$$G(\mathbf{x},\mathbf{x}';t-t_-)=\delta(\mathbf{x}-\mathbf{x}'). \tag{A9}$$

Let $\mathbf{k}=\mathbf{q}+k_z\mathbf{i}_z$. Equation (A8) then becomes[4]

$$G(\mathbf{x},\mathbf{x}';t-t')=\int_{-\infty}^{\infty}\frac{d\omega}{2\pi}\epsilon^{i\omega(t-t')}\int\frac{d\mathbf{q}}{(2\pi)^2}\frac{e^{i\mathbf{q}\cdot(\mathbf{r}-\mathbf{r}')}}{2[m(q,\omega)-1]}\exp(-\{z-z'+|z-z'|[m(q,\omega)-1]\}), \tag{A10}$$

where

$$m(q,\omega)=1+(1+i\omega+q^2)^{1/2}, \tag{A11}$$

with $\mathrm{Re}(1+i\omega+q^2)^{1/2}>0$.

We now multiply (A2) and (A6) with $G(\mathbf{x},\mathbf{x}';t-t')$ and $T(\mathbf{x}',t')$, respectively, add, and integrate in time and space,

$$\begin{aligned}
&\int_{-\infty}^{t_-}dt'\int d\mathbf{r}'\int_{-\infty}^{\infty}dz'\left[G(\mathbf{x},\mathbf{x}';t-t')\frac{\partial T(\mathbf{x}',t')}{\partial t'}+T(\mathbf{x}',t')\frac{\partial G(\mathbf{x},\mathbf{x}';t-t')}{\partial t'}\right]\\
&+\int_{-\infty}^{t_-}dt'\int d\mathbf{r}'\int_{-\infty}^{\infty}dz'[-G(\mathbf{x},\mathbf{x}';t-t')\nabla_{\mathbf{x}'}^2T(\mathbf{x}',t')+T(\mathbf{x}',t')\nabla_{\mathbf{x}'}^2G(\mathbf{x},\mathbf{x}';t-t')]\\
&+\int_{-\infty}^{t_-}dt'\int d\mathbf{r}'\int_{-\infty}^{\infty}dz'\left[-2G(\mathbf{x},\mathbf{x}';t-t')\frac{\partial T(\mathbf{x}',t')}{\partial z'}-2T(\mathbf{x}',t')\frac{\partial G(\mathbf{x},\mathbf{x}';t-t')}{\partial z'}\right]\\
&+\int_{-\infty}^{t_-}dt'\int d\mathbf{r}'\int_{\zeta(\mathbf{r}',t')}^{\infty}dz'2\lambda G(\mathbf{x},\mathbf{x}';t-t')\mathbf{v}(\mathbf{x}',t')\cdot\nabla_{\mathbf{x}'}T(\mathbf{x}',t')=0,
\end{aligned} \tag{A12}$$

where the lower limit for the z' integration in the last term is $\zeta(\mathbf{r}',t')$ since the velocity $\mathbf{v}$ is zero for $z'<\zeta(\mathbf{r}',t')$.

By grouping similar derivatives together and applying Green's second theorem to the second term in the left-hand side of (A12), we get

$$\begin{aligned}
&\int_{-\infty}^{t_-}dt'\int d\mathbf{r}'\int_{-\infty}^{\infty}dz'\frac{\partial}{\partial t'}[G(\mathbf{x},\mathbf{x}';t-t')T(\mathbf{x}',t')]\\
&+\int_{-\infty}^{t_-}dt'\int d\Gamma'\hat{\mathbf{n}}'\cdot[G(\mathbf{x},\mathbf{x}_{\Gamma'}(\mathbf{r}',t');t-t')\nabla_{\mathbf{x}'}T(\mathbf{x}',t')-T(\mathbf{x}',t')\nabla_{\mathbf{x}'}G(\mathbf{x},\mathbf{x}_{\Gamma'}(\mathbf{r}',t');t-t')]\\
&-2\int_{-\infty}^{t_-}dt'\int d\mathbf{r}'\int_{-\infty}^{\infty}dz'\frac{\partial}{\partial z'}[G(\mathbf{x},\mathbf{x}';t-t')T(\mathbf{x}',t')]\\
&+2\lambda\int_{-\infty}^{t_-}dt'\int d\mathbf{r}'\int_{\zeta(\mathbf{r}',t')}^{\infty}dz'G(\mathbf{x},\mathbf{x}';t-t')\mathbf{v}(\mathbf{x}',t')\cdot\nabla_{\mathbf{x}'}T(\mathbf{x}',t')=0.
\end{aligned} \tag{A13}$$

The second term represents integration over a surface *enclosing* the interface and placed at an infinitesimal distance from it.

Next, the z' integration in the third term of (A13) is performed so that the term becomes

$$-2\int_{-\infty}^{t_-}dt'\int d\mathbf{r}'[\lim_{z_1\to\infty}G(\mathbf{x};\mathbf{r}',z_1;t-t')T(\mathbf{r}',z_1,t')-\lim_{z_1\to-\infty}G(\mathbf{x};\mathbf{r}',z_1;t-t')T(\mathbf{r}',z_1,t')].$$

From (A3) we know that the temperature vanishes as $z\to\infty$ and thus the first term in the expression vanishes. The temperature reaches a constant value at $z\to-\infty$ and can be taken out of the integral sign so the remaining integral is

$$\int_{-\infty}^{t_-}dt'\int d\mathbf{r}'\lim_{z_1\to\infty}G(\mathbf{x};\mathbf{r}',z_1;t-t').$$

Using (A11) and the fact that

$$\lim_{c\to 0+}G(\mathbf{x},\mathbf{x}';-c)=0,$$

the integral can be written as

$$\lim_{z_1\to\infty}\int_{-\infty}^{\infty}dt'\int d\mathbf{r}'\int_{-\infty}^{\infty}\frac{d\omega}{2\pi}e^{i\omega(t-t')}\int\frac{d\mathbf{q}}{(2\pi)^2}\frac{e^{i\mathbf{q}\cdot(\mathbf{r}-\mathbf{r}')-(z-z_1)[2-m(q,\omega)]}}{2[m(q,\omega)-1]}=0\ .$$

Thus, the third term in (A13) does not survive even if the temperature at negative infinity is nonzero.

We can now perform the time integration in the first term of (A13),

$$\int d\mathbf{r}'\int_{-\infty}^{\infty}dz'\{G(\mathbf{x},\mathbf{x}';t-t_-)T(\mathbf{x}',t_-)-\lim_{t'\to-\infty}[G(\mathbf{x},\mathbf{x}';t-t')T(\mathbf{x}',t')]\}\ .$$

With the help of (A9) and the fact that

$$\lim_{t'\to-\infty}G(\mathbf{x},\mathbf{x}';t-t')=0\ ,$$

this integral becomes

$$\int d\mathbf{x}'\delta(\mathbf{x}-\mathbf{x}')T(\mathbf{x}',t_-)=T(\mathbf{x},t)\ , \tag{A14}$$

where t_- has been replaced by t since the temperature is a continuous function of time.

Returning to (A13), we find

$$\begin{aligned}T(\mathbf{x},t)=&\int_{-\infty}^{t_-}dt'\int d\Gamma'\hat{\mathbf{n}}'\cdot[G(\mathbf{x},\mathbf{x}_{\Gamma'}(\mathbf{r}',t');t-t')\nabla_{\mathbf{x}'}T(\mathbf{x}',t')-T(\mathbf{x}',t')\nabla_{\mathbf{x}'}G(\mathbf{x},\mathbf{x}_{\Gamma'}(\mathbf{r}',t');t-t')]\\&+2\lambda\int_{-\infty}^{t_-}dt'\int d\mathbf{r}'\int_{\zeta(\mathbf{r}',t')}^{\infty}dz'G(\mathbf{x},\mathbf{x}';t-t')\mathbf{v}(\mathbf{x}',t')\cdot\nabla_{\mathbf{x}'}T(\mathbf{x}',t')\ .\end{aligned} \tag{A15}$$

Since the domain Ω is infinite, we assume it is bounded by a surface that has been removed to infinity. Langer[15] has shown that in the absence of external fluxes, the contribution of this outer surface to the second term of (A15) is zero. Hence we restrict our attention to the crystal-melt interface Γ. The surface integral in (A15) contains the boundary values of the temperature and its normal derivative, and the continuity of the temperature implies that the term proportional to the gradient of the Green's function cancels out. We can now evaluate the remaining term, proportional to the normal component of the temperature gradient, using (A5),

$$\begin{aligned}T(\mathbf{x},t)=&\int_{-\infty}^{t_-}dt'\int d\mathbf{r}'[2+\zeta(\mathbf{r}',t')]G(\mathbf{x},\mathbf{x}_{\Gamma'}(t');t-t')\\&-2\lambda\int_{-\infty}^{t_-}dt'\int d\mathbf{r}'\int_{\zeta(\mathbf{r}',t')}^{\infty}dz'G(\mathbf{x},\mathbf{x}';t-t')\mathbf{v}(\mathbf{x}',t')\cdot\nabla_{\mathbf{x}'}T(\mathbf{x}',t')\ ,\end{aligned} \tag{A16}$$

since for *single valued* $z=\zeta(\mathbf{r},t)$

$$\hat{\mathbf{n}}\cdot\mathbf{i}_z d\Gamma=d\mathbf{r}=r\,dr\,d\varphi\ .$$

Equation (A16) is the integral equivalent of the transient convective-diffusion equation in the moving coordinate system. In the case of a steadily propagating interface, i.e., with a uniform velocity equal to that of the coordinate system, (A16) reduces to the *steady-state* equation

$$\begin{aligned}T(\mathbf{x})=&\,2\int d\mathbf{r}'G_{ss}(\mathbf{x},\mathbf{x}_{\Gamma'})\\&-2\lambda\int d\mathbf{r}'\int_{\zeta(\mathbf{r}')}^{\infty}dz'G_{ss}(\mathbf{x},\mathbf{x}')\mathbf{v}(\mathbf{x}')\cdot\nabla_{\mathbf{x}'}T(\mathbf{x}')\ .\end{aligned} \tag{A17}$$

Here $G_{ss}(\mathbf{x},\mathbf{x}')$ represents the Green's function that corresponds to steady diffusion in the moving coordinate system and is given by

$$G_{ss}(\mathbf{x},\mathbf{x}')=\int_{-\infty}^{t_-}dt'G(\mathbf{x},\mathbf{x}';t-t')\ . \tag{A18}$$

The integral equation that corresponds to the *one-sided* model is identical to (A16) for zero surface tension since there is no flux through the isothermal solid. In the presence of surface tension, the convective effects are represented by a term identical to that in (A17). On the other hand, the diffusive contribution is now different since heat cannot flow through the solid ($\alpha_s=0$). The derivation of the corresponding diffusion term has been presented by Caroli *et al.*[4]

[1]D'Arcy Thompson, *On Growth and Form* (Cambridge University Press, Cambridge, 1917).
[2]G. P. Ivantsov, Dokl. Akad. Nauk SSSR **58**, 567 (1947).
[3]J. S. Langer, Rev. Mod. Phys. **52**, 1 (1980).
[4]B. Caroli, C. Caroli, B. Roulet, and J. S. Langer, Phys. Rev. A **33**, 442 (1986).
[5]J. S. Langer, Phys. Rev. A **33**, 435 (1986).
[6]D. I. Meiron, Phys. Rev. A **33**, 2704 (1986).
[7]D. A. Kessler, J. Koplik, and H. Levine, Phys. Rev. A **33**, 3352 (1986).
[8]D. A. Kessler and H. Levine, Phys. Rev. Lett. **57**, 3069 (1986).
[9]M. E. Glicksman and S. C. Huang (unpublished); M. E. Glicksman and S. C. Huang (unpublished); S. C. Huang and M. E. Glicksman, Acta Metall. **29**, 701 (1981).
[10]We are aware of one other rigorous analysis of a situation in which flow is present. G. B. McFadden and S. R. Coriell, J. Cryst. Growth **74**, 507 (1986), analyzed the situation where the density change upon solidification engenders flow.

[11]P. Pelce and Y. Pomeau, Stud. Appl. Math. **74**, 245 (1986).

[12]Wilkinson, Q. J. Mech. Appl. Math. **8**, 415 (1955), worked out the solution to the Oseen problem for a general paraboloid. Our results can readily be extended to cover the solidification of a paraboloidal crystal. There it is somewhat easier to recast the problem in terms of differential equations from the outset. We have used the integral formulation here to simplify the development of a model that will describe the temporal evolution of interfaces where interfacial tension is important.

[13]R. T. Davis and M. J. Werle, AIAA J. **10**, 1224 (1972).

[14]J. Wilkinson, Q. J. Mech. Appl. Math. **8**, 415 (1955).

[15]J. S. Langer, Acta Metall. **25**, 12 (1977).